Role of Entrance-channel Dynamics in Heavy Element Synthesis

D. J. Hinde,* A. C. Berriman, R. D. Butt, M. Dasgupta, I. I. Gontchar,† C. R. Morton, A. Mukherjee, and J. O. Newton

Department of Nuclear Physics, Research School of Physical Science and Engineering, Australian National University, Canberra, ACT 0020, Australia

Received: November 13, 2001; In Final Form: April 17, 2002

In heavy element synthesis, the population surviving quasi-fission and fusion-fission is far out in the tail of the distribution of reaction outcome probabilities, and should be sensitive to slight changes in the reaction conditions. Because of the extremely low yields of very heavy elements, it is difficult to make detailed and systematic experimental studies. However, studies of less-fissile systems can give valuable information relevant to the formation of super-heavy elements. Measurements made at the ANU, Canberra, to study the influence of entrance-channel properties on the subsequent reaction dynamics are presented. New and surprising data show that the entrance-channel mass-asymmetry plays a role in the compound nucleus formation probability, even when forming a nucleus as light as ^{216}Ra. The influence of different physical configurations, related to different contact barrier energies, on superheavy element formation is discussed.

1. Introduction

In planning experiments aimed at heavy element synthesis, prediction of absolute cross sections without extrapolation from nearby experimental cross sections is very challenging. This is due to the extreme complexity of the process, and the very low probability of evaporation residue (ER) formation. In the distribution of reaction outcome probabilities, the population surviving the competing quasi-fission and fusion-fission processes is far out in the tail, and thus would be expected to be extremely sensitive to slight changes in the reaction conditions. Because of the very low yields, it is difficult and time-consuming to make detailed and systematic experimental studies for the reactions actually leading to very heavy, or super-heavy nuclei. However, such studies for reactions forming less fissile nuclei are more feasible, and can give valuable information on the dynamical processes occurring during the fusion of two nuclei, which will also be relevant to reactions forming super-heavy elements.

The calculation of the cross section for formation of a super-heavy element can conceptually be divided into three parts. In reality these are not independent of each other, but are still sufficiently distinct to constitute a useful framework for discussion. Firstly, the cross section for contact of the two colliding nuclei must be determined. Contact may be defined as a configuration where complex nuclear reactions between the two nuclei become highly probable. For light systems, this is at a radius inside the peak in the potential barrier (capture barrier, or fusion barrier), and automatically leads to a compact compound nucleus. For collisions of heavier nuclei, this must be multiplied by the probability (less than unity) of reaching a compact shape inside the unconditional fission barrier. Those collisions which do not achieve this compact shape contribute to the quasi-fission or deep-inelastic yield. For those composite nuclei achieving a compact shape, the yield of the evaporation residues is determined by the probability of surviving fission decay from this compact configuration. The identity of the nuclei reaching the compact shape will be dependent on particle evaporation during the dynamical phase. Thus the evaporation residue (ER) formation cross section may be written:

$$\sigma_{\rm ER}(E^*,l) = \sigma_{\rm contact}(E^*,l,EC)\cdot P_{\rm compact}(E^*,l,EC)\cdot P_{\rm surv}(E^*,l) \quad (1)$$

where $\sigma_{\rm contact}(E^*,l,EC)$ is the cross section for capture, for excitation energy E^* of the heavy nucleus with angular momentum $l\hbar$, and in general depends on specific entrance channel (EC) conditions. $P_{\rm compact}(E^*,l,EC)$ is the probability of passing to a compact shape, and $P_{\rm surv}(E^*,l) = [1 - P_{\rm fis}(E^*,l)]$ is the survival probability against fission from the compact shape. It is re-emphasised that in reality, the nucleus will cool by evaporation during the transition to the compact shape, so the latter two factors are not independent. $P_{\rm compact}(E^*,l,EC)$ is complementary to the probability of quasi-fission $P_{\rm QF}(E^*,l,EC)$, namely $P_{\rm compact} + P_{\rm QF} = 1$. To maximise the heavy nucleus survival cross section, the product of all three factors must be maximised. As will be discussed in detail, the physical processes associated with the entrance channel can make it impossible to simultaneously maximise all three factors individually, thus the choice of reaction is in practice a trade-off of one factor against the other. This can be seen in the similar yields of heavy elements in cold fusion[1] and hot fusion[2,3] reactions. Specific entrance channel effects will be discussed in the next sections.

2. Contact of Two Nuclei

2.1. Entrance Channel Barrier Distribution. It is by now well-established that in collisions of heavy nuclei, there is not a single potential barrier, but a distribution of barrier energies,[4] where $D(E)$ is defined as the probability of encountering a barrier of energy E, and can be determined directly from experimental capture cross sections closely-spaced in energy.[5,6] The distribution can be understood classically in the case of statically-deformed nuclei, where different orientations of the deformation axis with respect to the incident projectile result in potential barriers at different radii, and thus energy.[6] Strongly-coupled collective vibrations (quadrupole[7] and octupole[8]), and multi-nucleon transfer, can also give rise to broad barrier distributions. Typically, the width of the barrier distribution is between 5% and 10% of the mean barrier energy.[9] Although these different barriers affect all reaction processes, here we are particularly interested in capture (or fusion, for lighter systems).

For systems light enough that quasi-fission is not present, all the nuclei which pass inside the potential barrier(s) lead to an equilibrated compound nucleus. It is possible to identify the sum of the fission and evaporation residue yields with passage inside the capture barrier(s), and thus the term fusion barrier distribution is appropriate in this regime. For heavier systems, though the two nuclei may be captured inside the potential barrier, they are likely to re-separate after energy damping and mass-exchange (deep inelastic or quasi-fission processes). In

*Corresponding author. E-mail: David.Hinde@anu.edu.au. FAX: +61-2-6125-0748.

†Permanent address: Omsk State Railway University, pr.Marksa 35, Omsk, 644046 Russia.

Published on Web 6/30/2002

such cases, the entrance-channel model describes the capture cross sections, and so we refer to the capture barrier distribution. It is important to appreciate that entrance channel models should not be compared with evaporation residue yields in such cases, since the capture cross section is only one of the factors in eq 1 which defines the ER cross sections. Similarly, a dynamical model describing the probability of passing to the compact configuration, but neglecting the dynamics in the entrance channel may also result in misleading conclusions.

The presence of the wide capture barrier distributions which necessarily occur during the collision of two heavy nuclei (due to the high charge product), should constitute a significant element in interpretations or predictions of cross sections for reactions forming super-heavy nuclei. In general, reactions at energies below the uncoupled potential barrier occur not through tunneling through that barrier, but by passage over a lower barrier, which is encountered with a probability defined by the barrier distribution. In the language of Myers and Swiatecki,[10] those collisions which actually lead to very heavy nuclei are almost certainly "unshielded", the capture barrier having been below the bombarding energy. The fact that there is almost no potential pocket for the uncoupled barrier will surely influence the extent and probability of finding barriers at energies lower than the uncoupled barrier, but lower barriers will exist. To maximise ER cross sections, not only should the weights (probabilities) of these lower barriers be maximal, but the elongation of the composite nucleus at contact, after passing the potential barrier, should be as small as possible. The latter point is illustrated below from experimental measurements.

3. Dependence of Quasi-fission Competition on Contact Configuration

3.1. Quasi-fission Measurements. Generally, different potential barriers correspond to different conditions or configurations of the two nuclei at the capture barrier radius. The question then arises, does the configuration at the capture barrier radius influence the outcome of the reaction? If an equilibrated compound nucleus is always formed, according to Bohr's independence hypothesis, the answer should be no. If this is not the case, as in quasi-fission, some influence could in general be expected. From the discussion of eq 1, it may seem that there are two complementary methods of experimentally investigating this question, which should give the same information. The first is to look for changes in the fission properties indicating the presence of quasi-fission, whilst the second is to investigate inhibition of the evaporation residue yields. The situation is not quite so simple, however, since the general dependence of the fission process on angular momentum could result in quasi-fission competing with fusion at high angular momenta, resulting only in suppression of fusion-fission, but not affecting the evaporation residue yields which arise from the lower angular momenta. This question will be addressed in sect. 4.3 and 4.4.

A number of experimental studies have been made which have been interpreted as showing that, for a given reaction, the quasi-fission probability depends on the conditions at the capture barrier. The first such data interpreted in this way was for the reaction $^{16}O + ^{238}U$, where the fission anisotropy was observed to rise dramatically as the beam energy fell through the capture barrier region, which can be seen by comparing Figure 1(a) and (c). In that work, it was proposed that fusion at the lowest beam energies, which results exclusively from the projectile approaching the tips of the prolate deformed target nuclei, leads preferentially to quasi-fission. Qualitatively, this picture could explain the trend of the data. There was also a small asymmetry in the fission mass-distribution, which became more pronounced at the same beam energy as the change in the anisotropy, as shown in Figure 1(b).

The hypothesis that $P_{QF}(E^*, l, EC)$ depends on the orientation of the heavy deformed nucleus as the projectile reaches the capture barrier could be specific to heavy nuclei with a large static deformation. Alternatively, it could be a reflection of universal behaviour in heavy nucleus-nucleus collisions, in which low capture barriers (which are generally associated with large barrier radii) could always result in enhanced quasi-fission, with concomitant suppression of fusion.

To investigate this important question, a comparison of two reactions already known[11,12] to have substantial quasi-fission probabilities was made. The two reactions compared were $^{32}S + ^{208}Pb$ (where ^{208}Pb is spherical) and $^{32}S + ^{232}Th$ (where ^{232}Th is prolate deformed). Recent measurements at the Australian National University (ANU) mapped out the detailed behaviour of the fission properties across the capture barrier energy region. Figure 2 shows the capture barrier distributions, the centroids of the fission mass distributions measured at a back-

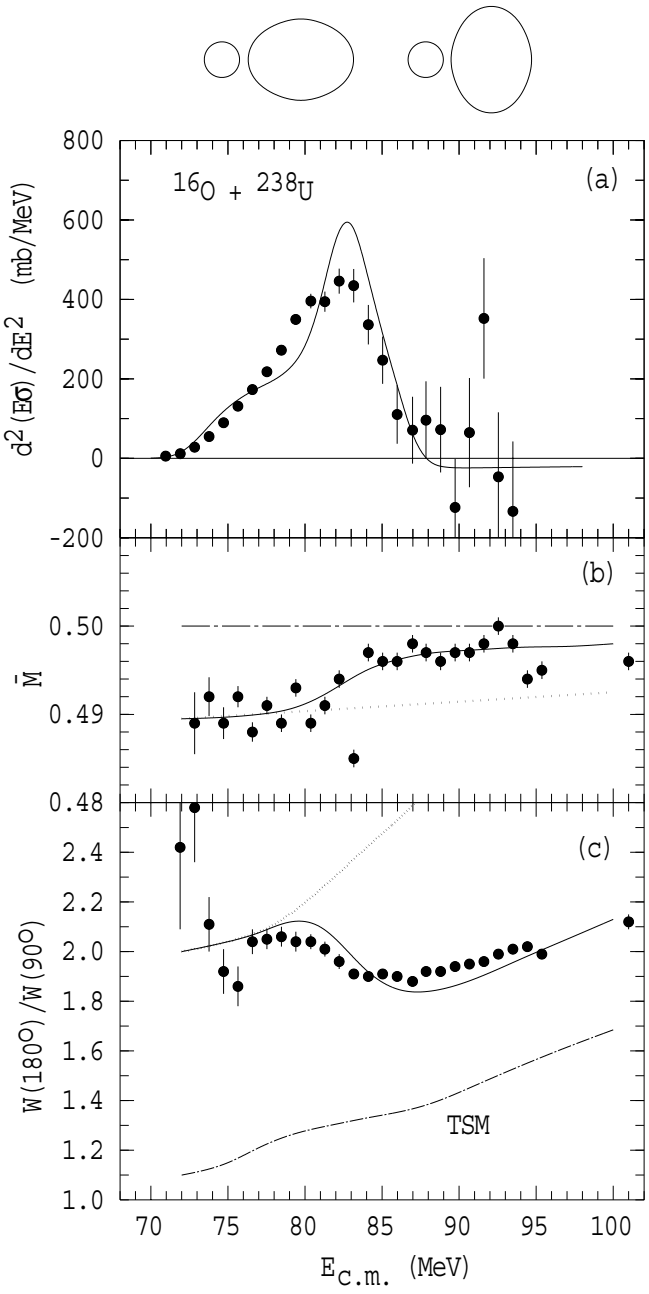

Figure 1. (a) The capture barrier distribution for $^{16}O + ^{238}U$ together with a model calculation. (b) The measured centroids of the fission mass-splits (symmetric fission is indicated by the dot-dashed line). (c) The energy dependence of the fission anisotropy. In panels (b) and (c), the predictions of the TSM with the inclusion of couplings in capture are given by the dot-dashed lines, whilst the assumption for pure quasi-fission is given by the dotted lines. The predictions of the orientation dependent quasi-fission model based on these values are indicated by the full lines.

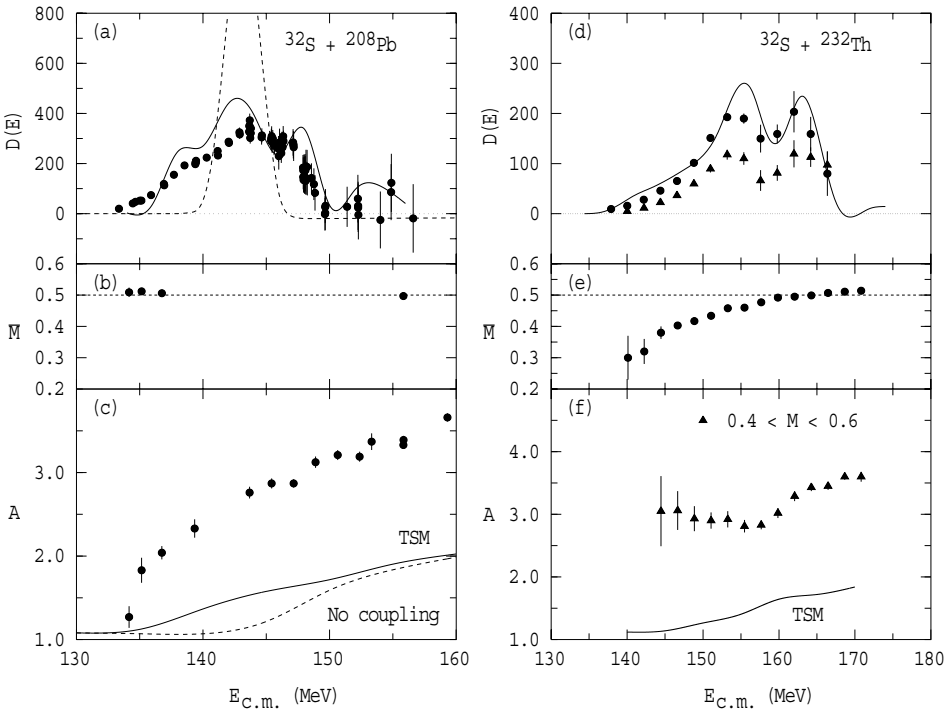

Figure 2. The barrier distribution (a) for $^{32}S + ^{208}Pb$ together with (b) the centroids of the fission mass-splits (symmetric fission is indicated by the dashed line) and (c) the energy dependence of the fission angular anisotropy. The predictions of the TSM with and without the inclusion of couplings in capture are given by the dashed and full lines respectively. Similar quantities for $^{32}S + ^{232}Th$ are shown in (d), (e), and (f), the results for symmetric mass-splits between 0.4 and 0.6 of the compound nucleus mass being indicated by triangles. For both reactions, coupled-channels calculations of the capture barrier distributions show that the inclusion of wide barrier distributions does not allow reproduction of the measured anisotropy values.

ward angle, and the anisotropies as a function of beam energy for each reaction. In both cases, the anisotropies calculated assuming fusion-fission using the transition state model (labeled TSM) are small, whether the width of the barrier distribution is included (full lines) or not (dashed lines). These anisotropies are small because the calculated saddle-point shapes are very compact for such fissile compound nuclei, allowing fission far from the plane normal to the angular momentum vector.

For both reactions, the measured anisotropies A lie well above the calculations, indicating that the fission occurs close to the plane normal to the angular momentum vector. This implies that compact shapes are not generally reached in these reactions, consistent with previous conclusions[11,12] that quasi-fission predominates. The energy dependence of A for the two reactions is, however, very different. For $^{32}S + ^{232}Th$, A rises as the energy falls below the average fusion barrier energy, as observed for lighter projectiles incident on deformed heavy targets, for example $^{16}O + ^{238}U$ (Ref. 14) and even $^{12}C + ^{238}U$,^{232}Th (Ref. 15, 16). In contrast with the reactions induced by lighter projectiles, which only show small changes (see Figure 1(b)), the energy dependence of the shape of the fission mass-distributions for $^{32}S + ^{232}Th$ shows marked changes in shape and centroid, as demonstrated in Figure 2(e). For $^{32}S + ^{208}Pb$, however, the anisotropy falls monotonically with decreasing energy, and the mass-distributions show essentially no change in shape or centroid, unlike those for the ^{232}Th target. Thus there is no indication in the $^{32}S + ^{208}Pb$ data of a significant change in the character or probability of quasi-fission which is dependent on the energy of the barrier encountered, unlike reactions with statically deformed heavy nuclei. This is most likely correlated with the high frequency of the vibrational excitations of ^{208}Pb, as opposed to the low frequency associated with collective rotational excitations of ^{232}Th.

In reactions involving heavy statically deformed nuclei, the configuration found at the capture barrier is likely to remain essentially unchanged up to the time the two nuclei start to merge together, and so influences the subsequent fission dynamics. For vibrational nuclei, a configuration resulting in a low energy fusion barrier will not necessarily translate into an elongated composite nucleus, due to the high frequency of the collective vibrational modes.

3.2. Dependence of Evaporation Residue Yield on Contact Configuration. The energy dependence of the fission behaviour in the two ^{32}S-induced reactions discussed above thus indicates a specific influence of static deformation of the system before contact on the subsequent reaction dynamics. A general increase in quasi-fission associated with contact barriers with larger radii (lower energy) than average is not indicated. The data do support the hypothesis originally developed to explain the anisotropies for the $^{16}O + ^{238}U$ reaction. At that time, it was suggested that the orientation-dependence of the quasi-fission probability would lead to suppression of evaporation residue yields at sub-barrier energies, whilst it may lead to enhancement at above-barrier energies. In terms of eq 1, this occurs because the orientation-dependence of the quasi-fission probability also defines the complementary probability $P_{\mathrm{compact}}(E^*, l, EC)$ of reaching the equilibrium deformation.

Recently, measurements of evaporation residue cross sections have been made at JAERI, for the $^{60}Ni + ^{154}Sm$ (Ref. 17) and $^{76}Ge + ^{150}Nd$ (Ref. 18) reactions, where both target nuclei have large prolate static deformations. It was found that there was essentially no evaporation residue yield in the lowest 10 MeV of the calculated fusion barrier distribution, corresponding only to those collisions where the projectile makes contact with the tip of the target nuclei. This result, complementary to studies of fission properties in the same low energy regime, is consistent with the above picture of orientation-dependent quasi-fission.

4. Dependence of Quasi-fission on Entrance Channel Mass-asymmetry

It has long been recognised that the probability of quasi-fission depends on the entrance-channel mass-asymmetry. A number of comparative measurements, where the same compound nucleus has been formed with different pairs of projectile and target nuclei, have shown[19,20] that for the reaction with the more symmetric entrance-channel masses, the fission properties show signatures characteristic of quasi-fission (for example, broader mass distributions).

A recent study at the ANU, reported in Reference 21, showed for the first time the presence of quasi-fission, and the simultaneous suppression of the evaporation residue yield, for mass-asymmetric reactions. These results are described below.

4.1. ANU Experimental Studies of Reactions Forming ^{216}Ra. Three combinations of projectile and target nuclei were used to form ^{216}Ra: ^{12}C + ^{204}Pb, ^{19}F + ^{197}Au, and ^{30}Si + ^{186}W. The evaporation residue (ER) cross sections were measured, as well as the fission cross sections and properties. Although the fission may previously have been expected in such reactions to result only from fusion-fission, in principle it also includes contributions from the quasi-fission process (if present) in which no evaporation residues are produced. Measurements were made at ten or more beam energies, from the Coulomb barrier upwards for each reaction. The energies were chosen such that the ^{216}Ra nuclei were formed at the same excitation energy in the three reactions.

The 14UD tandem electrostatic accelerator at the ANU provided pulsed beams which bombarded thin isotopically enriched targets. The ^{204}Pb target was enriched to 99.7%, which was confirmed by the absence of α lines from the lighter Pb isotopes. To determine the cross sections for ERs, aluminum catcher foils were placed immediately behind the target to stop the ERs.[22] The catcher foils were 1.5–2.5 times thicker than the average range of the ERs for each reaction. All the ERs undergo subsequent α decay from their ground-states, with lifetimes from 1.9 s to 3.5 h. The α particles resulting from the decay were detected in an annular solid-state detector as shown in Figure 3(a). Repeat measurements for the ^{30}Si reaction with a thicker catcher gave the same cross sections, confirming that all ERs were stopped. Measurements were made both during and after irradiation. Together with the use of a sophisticated peak-fitting program, this allowed determination of the individual yields of almost all evaporation channels

Measurements of fission were carried out in separate experiments, the two fission fragments being detected in two large area, position-sensitive multi-wire proportional counters arranged as shown in Figure 3(b). Each covered an angular range of 75°, allowing determination of the cross section in a single measurement. The coincident detection of both fragments allowed the determination of the fission fragment mass-ratio through reconstruction of the velocity ratio.[14]

In both ER and fission measurements, cross sections were determined by normalizing to the yields of elastically scattered beam particles measured in monitor detectors located at ±22.5°. It was essential that reliable *absolute* cross sections were obtained in order to make meaningful comparisons between reactions. This could be achieved, without requiring determination of transmission efficiencies through a complex apparatus, because the cross sections were sufficiently large that the ERs could be identified when stopped *at the target location*. Thus accurate absolute detector normalisation could be obtained simply by measuring elastic scattering both in the monitor detectors and in the α-particle and fission detectors, at low beam energies where the elastic scattering cross sections will be Rutherford. The individual ERs, identified by their decay α-particle energies and lifetimes, were mainly Ra isotopes, formed after the emission of $x = 3, 4, 5, \ldots$ neutrons.

4.2. Experimental Results for ^{216}Ra. The ratio of the yield of a given *xn* channel to the total *xn* cross section was determined at each energy for the three reactions, the results being shown in Figure 4, as a function of excitation energy in ^{216}Ra. Bohr's independence hypothesis[23] states that compound nuclei with the same excitation energy and angular momentum will decay independently of their method of formation. The data show that for the ER, this is the case, the peak in the ER yield for each isotope occurring at a value of E^* essentially independent of the reaction. This confirms that the actual excitation energies of the ^{216}Ra nuclei formed in the three reactions are indeed essentially the same, and that pre-equilibrium neutron emission is not significant, as expected at low beam energies.

The sum of the fission and ER cross sections defines the capture cross section. Both are shown, for all three reactions, in Figure 5 and Figure 7(a). In each case, the ER cross sections peak at a certain beam energy, then fall, whilst the contribution

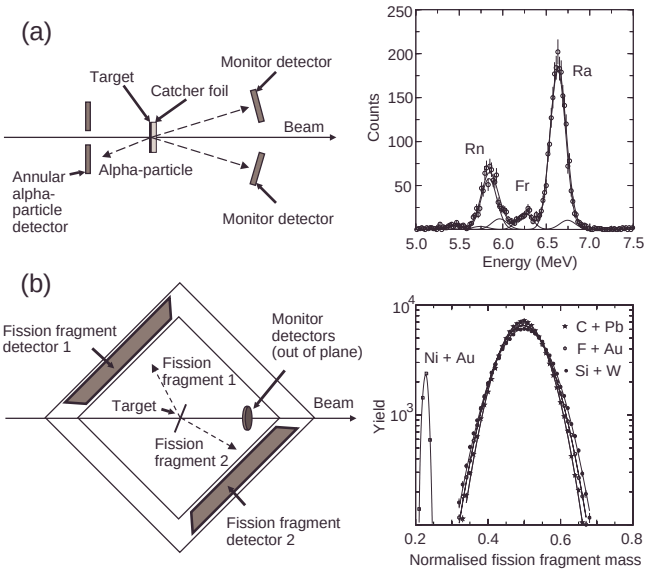

Figure 3. Experimental configurations for the two types of measurement and typical measured spectra. (a) A schematic diagram of the configuration of the ER measurements with a typical α-particle energy spectrum from the annular α-particle detector, and the fit to the spectrum (full lines). This spectrum shows that the α particles from Ra can be very clearly identified. (b) Configuration for the fission measurements, with three normalized mass spectra (defined as the mass of one fragment divided by the total mass) measured for fission of ^{216}Ra at the same excitation energy in the three reactions. The peak for elastic scattering of ^{58}Ni from ^{197}Au shows the good experimental resolution.

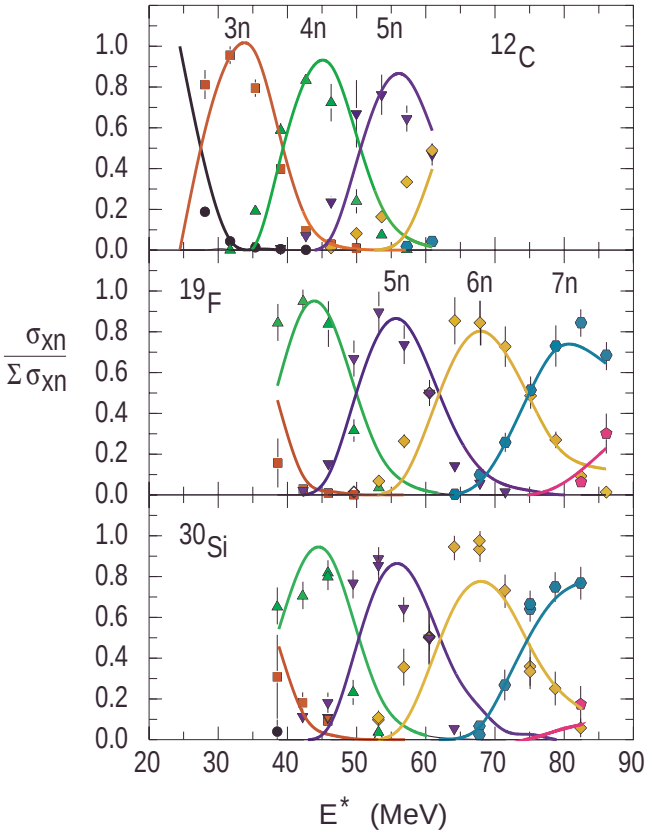

Figure 4. The ratio of individual *xn* channel cross sections to the total *xn* cross section, for the three reactions forming ^{216}Ra. Statistical model calculations are shown by the curves. The *xn* excitation functions are almost identical in the three reactions.

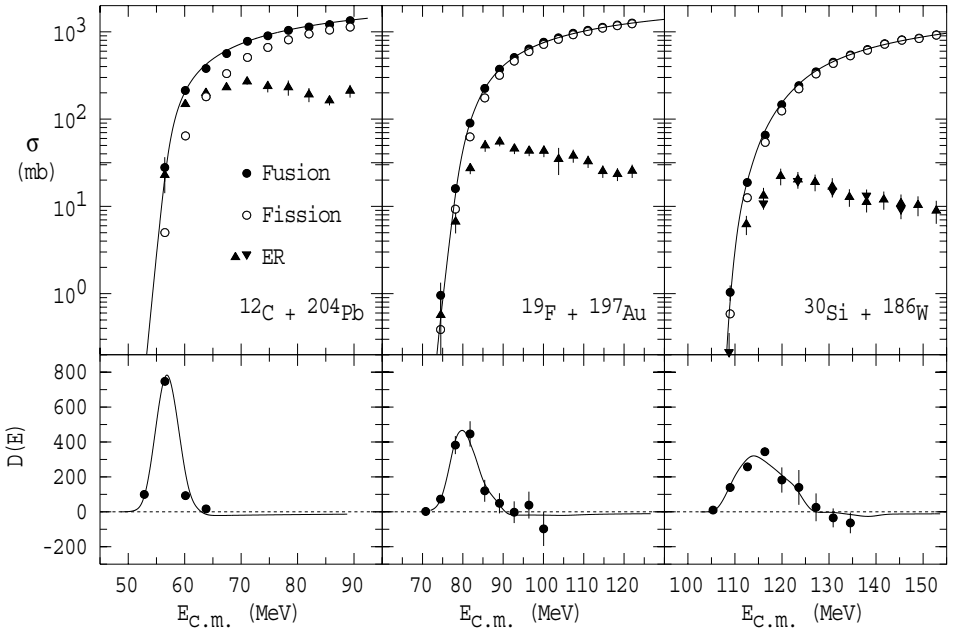

Figure 5. cross sections and capture barrier distributions for the three reactions $^{12}C + ^{204}Pb$, $^{19}F + ^{197}Au$, and $^{30}Si + ^{186}W$. The upper frames show the sum (closed circles) of the measured fission (open circles) and ER (triangles) cross sections. For the $^{30}Si + ^{186}W$ reaction the different triangle symbols represent ER measurements using different stopper foil thicknesses. The lower panels show the experimental capture barrier distributions $D(E)$. The lines represent the results of the coupled-channels calculations using known target and projectile excitations.

of ERs to the capture cross sections decreases as the projectile becomes heavier. Calculations using nuclear potential parameters consistent with many other reactions,[9] and coupling parameters from the known properties of the collective modes in each nucleus, reproduced the present capture cross sections and barrier distributions $D(E)$ for the three reactions, typically to within 2%, indicating that the three systems behave as expected. These calculations are shown by the lines in Figure 5. From these calculations, the capture angular momentum distributions were obtained for each beam energy, for the three reactions. As the beam energy increases, the projectile can bring in higher angular momenta $l\hbar$. As the height of the fission barrier falls proportional to l^2, this leads to the observed rapid fall in the ER probability. Fitting these data with a statistical decay simulation shows that the fission probability exceeds 98% at $l = 30$. This restricts ER survival to low l values, allowing a simple and essentially model-independent comparison of the measured ER yields for the three reactions, which is described below.

4.3. Reduced ER cross sections $\tilde{\sigma}_{ER}$. At a given beam energy E, the total ER cross section is the sum of the cross sections from each l, these being the products of the capture cross sections and the probabilities of surviving fission $(1 - P_f(l, E^*))$. Initially it is assumed that $P_f(l, E^*)$ is independent of the entrance channel. Thus

$$\sigma_{ER}(E) = \pi\lambda\!\!\!^{-2} \sum_{l=0}^{\infty} (2l+1)\ T_l(E)\ (1 - P_f(l, E^*)), \qquad (2)$$

where $T_l(E)$ is the probability of capture for l, and $\lambda\!\!\!^{-}$ is the reduced deBroglie wavelength, determined by the beam momentum. Division by $\pi\lambda\!\!\!^{-2}$ gives the reduced cross section $\tilde{\sigma}_{ER}$. Although the coupled-channels capture models can reliably predict $T_l(E)$, reliance on a particular calculation can be eliminated. This is because all such models show that at beam energies sufficiently high above the Coulomb barrier, $T_l(E)$ is essentially unity for all l which lead to ERs. At these energies $T_l(E)$ can be dropped, giving

$$\tilde{\sigma}_{ER}(E) = \sum_{l=0}^{\infty} (2l+1)\ (1 - P_f(l, E^*)). \qquad (3)$$

Thus at the same E^*, the three reactions should give the same $\tilde{\sigma}_{ER}$, as long as $P_f(l, E^*)$ is independent of the reaction, in accordance with Bohr's hypothesis. Monte Carlo statistical model calculations[24] (using $T_l(E)$ from the coupled channels calculations which reproduced the measured capture cross sections) indeed show this behaviour, as illustrated in Figure 6(a), where the three lines corresponding to each reaction converge when all reactions fully populate the angular momenta leading to ERs ($T_l(E) = 1$ for all l below 30). By comparison, the experimental ER data do not converge, but show a systematic difference for each reaction, with the yield of ERs being largest for the light-

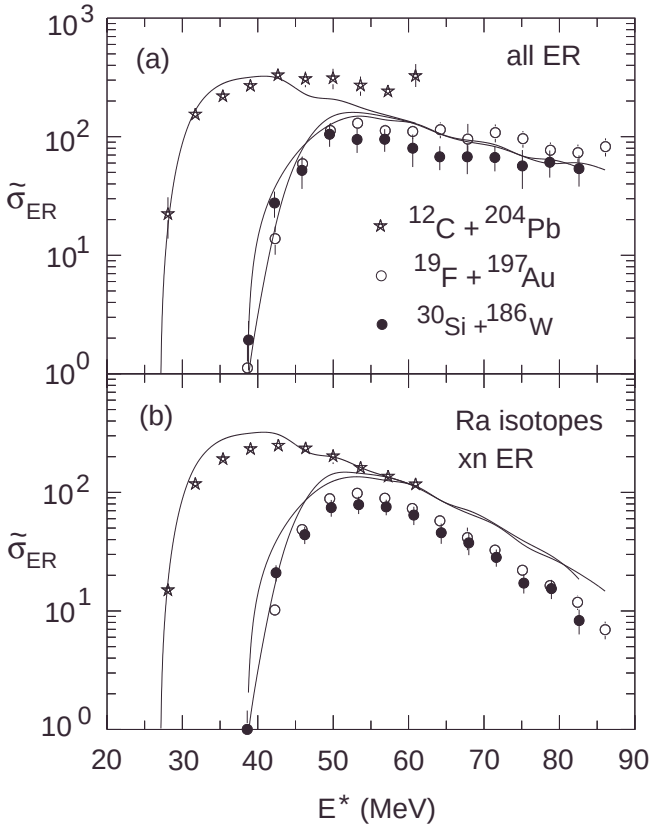

Figure 6. Reduced cross sections for ERs as a function of excitation energy for (a) all ERs and (b) radium ERs. Monte Carlo statistical model calculations, based on Bohr's independence hypothesis, are shown by the curves, which converge at the higher energies. In contrast, the measured ER reduced cross sections for the heavier projectiles are inhibited compared to those for ^{12}C.

est projectile. The yields could be affected by the recognized phenomenon of breakup of the lighter projectiles into α-particle clusters,[25] leading at high l to incomplete fusion, resulting in increased ER formation rather than fission. Contributions from incomplete fusion can be eliminated by summing the yields for Ra isotopes alone, which can only be formed when all the protons in the projectile are captured. These yields, plotted in Figure 6(b), still show a strong dependence on projectile mass, those for ^{19}F and ^{30}Si being respectively 0.64 ± 0.09 and 0.57 ± 0.08 of those for ^{12}C at the two highest energies. This cannot be explained by the low values of $T_l(E)$, since the measured capture cross sections for all three reactions can only be reproduced with $T_l(E)$ values close to unity. The only reasonable conclusion is that either $P_f(l, E^*)$ depends on the reaction, in disagreement with Bohr's hypothesis, or that fission is not all from the fully equilibrated compound nucleus. Then the right hand side of eq 2 must be multiplied by the probability of passing from the contact to the compact shape, as in eq 1, allowing for inhibition of true fusion for the heavier projectiles. Fusion with light projectiles (such as ^{19}F) has previously implicitly been assumed to proceed without any inhibition. We believe that this is the first observation of fusion inhibition for such a light projectile.

4.4. Fission Mass Distributions. If the inhibition is caused by the presence of quasi-fission, as in reactions forming superheavy nuclei, there should be evidence for quasi-fission in the fission mass-distributions, since quasi-fission is expected to have a broader mass-distribution than fusion-fission. The width of the fusion-fission mass-distribution depends principally on excitation energy, but may depend slightly on angular momentum. However, if the ^{216}Ra compound nuclei formed at the same E^* in different reactions have the *same* angular momentum distributions, then according to Bohr's hypothesis, the fission mass-distributions should be identical. The angular momentum distributions can be reliably predicted[26,27] by the coupled-channels calculations that reproduce the capture cross sections.[9] Figure 7(a) shows the dependence of the deduced mean l^2 on E^*. This demonstrates that the ^{12}C reaction matches the ^{30}Si reaction at one energy, and approaches the ^{19}F reaction at the highest energy. Qualitatively this must happen, as the heavier projectiles have a higher threshold E^* for capture, but carry more angular momentum than ^{12}C. The measured variances of the fission mass-distributions for the three systems, presented in Figure 7(b), do not match at any energy, but rather show a systematic dependence on projectile mass, as well as the expected increase with E^*. This result is consistent with the observed inhibition of fusion for the heavier projectiles, indicating an increasing contribution from the quasi-fission process, in which no ERs are produced, and for which full mass-equilibration is not expected, leading to wider mass-distributions for the reactions with heavier projectiles.

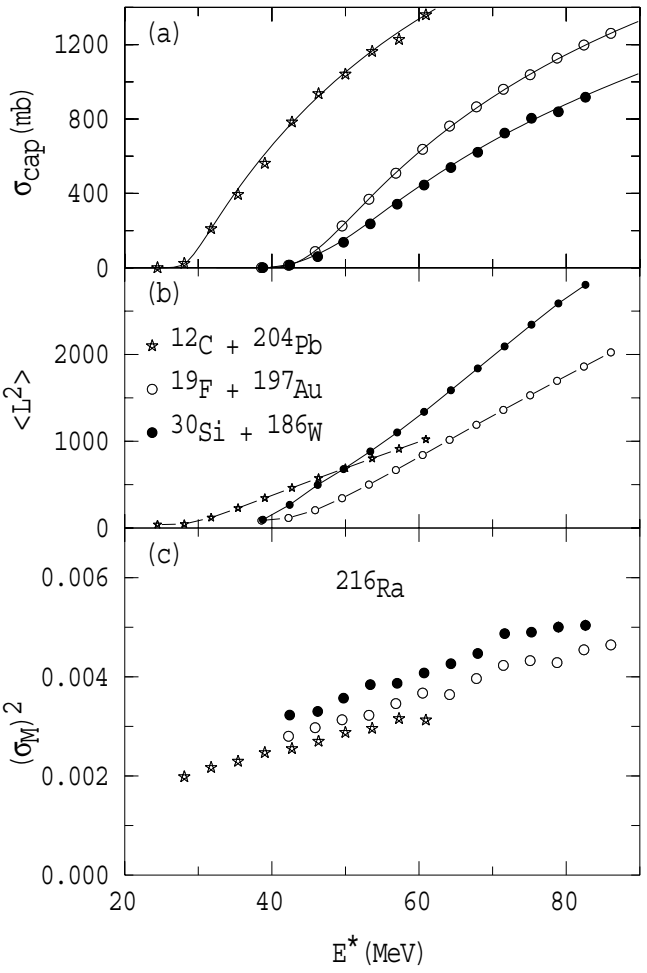

Figure 7. Experimental evidence for quasi-fission. As a function of excitation energy we present the measured and calculated capture cross sections for the three reactions, shown in panel (a), whilst the calculated mean-squared angular momentum introduced in the three reactions, based on these fits, are shown in panel (b). The measured variances of the normalized fission mass-distributions are shown in panel (c). Experimental uncertainties are typically smaller than the size of the points. For the same excitation energy and mean-squared angular momentum in ^{216}Ra, the mass distributions for the reactions are not the same. The systematic dependence of the variance on the mass-asymmetry of the projectile and target is evidence for an increasing contribution from quasi-fission associated with the projectile mass.

Having found convincing evidence for quasi-fission in the fission mass-distributions, as well as inhibition of fusion, we conclude that the combined results indicate that quasi-fission is not only competing with fusion-fission at high angular momenta, but is also competing at the low angular momenta leading to ERs.

4.5. Interpretation in terms of Entrance-channel Mass-asymmetry. These results may be interpreted qualitatively by considering what can happen to the projectile nucleus when it makes contact with the target nucleus. It may be swallowed up by the heavier nucleus, resulting in a compact compound nu-

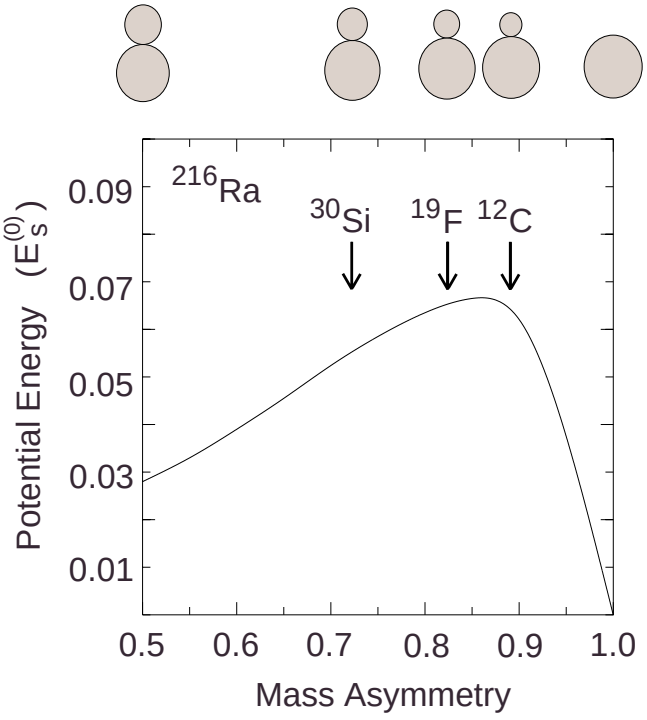

Figure 8. Fission barrier energies for ^{216}Ra are shown as a function of mass-asymmetry, defined as the difference between the masses of the two parts of the elongated nuclear system divided by their sum. The barrier energies, calculated with the Liquid Drop Model, are expressed in units of the spherical surface energy $E_s^{(0)}$ of ^{216}Ra. The initial mass-asymmetries for the three reactions are indicated. The shapes at contact corresponding to these asymmetries, and others, are sketched above.

cleus (fusion). Alternatively, it may gain mass from the heavier nucleus, and the system will approach the entrance channel configurations of more and more mass-symmetric collisions. Although it may still fuse from these configurations, passing inside the unconditional saddle-point deformation, the system may also separate, leading to quasi-fission.

Though this seems qualitatively to be a reasonable interpretation, we must consider an alternative explanation, related to the orientation dependent quasi-fission picture described above for statically deformed nuclei, where increased elongation of the system at contact increases the quasi-fission probability. ^{204}Pb is essentially spherical, and the small oblate deformation of ^{197}Au results in contact shapes only 2% longer than average at most. The larger prolate deformation of ^{186}W can result in contact shapes over 7% longer than average. The largest change in the effect of deformation is thus between ^{197}Au and ^{186}W, whilst the largest change in ER yields is between ^{197}Au and ^{204}Pb. Furthermore, the comparison of $\tilde{\sigma}_{ER}$ must be made at energies above the fusion barrier region, where all orientations of the deformed nucleus contribute. Hence this mechanism seems unlikely to explain the observed difference between the ^{204}Pb and ^{197}Au reactions.

Fusion and quasi-fission competition has previously been discussed in terms of the dependence of the calculated heights of the mass-asymmetric fission barriers,[28–30] or in terms of the mass-asymmetry dependence of the energy of the contact configurations.[31] In Figure 8 the conditional fission barrier energies (interpolated from calculations of Reference 32) for ^{216}Ra are shown as a function of the mass-asymmetry. The projectile will tend to be absorbed if the mass-asymmetry is to the right of the peak, whilst if to the left, it will preferentially gain mass. The three reactions studied span the peak, with only the ^{12}C reaction on the side favouring rapid compound nucleus formation. It may seem surprising initially that the calculated potential energies for the fission shapes appear to agree so well with the experimental data, as the potential maximum for the contact shapes (which are less elongated than the conditional fission saddle-point shapes) occurs at smaller asymmetries. However, after contact, the development of a neck between the two nuclei causes the potential maximum to shift back to larger asymmetry,[33] similar to that found for the saddle-point shapes. Our results are consistent with the mass-asymmetry being a crucial variable determining the dynamics of these reactions, though of course the dynamics will not only depend on the the potential energy surface, but also on the dissipation and inertia tensors. A quantitative understanding of the effect of mass-asymmetry, and other important variables such as the deformation of the symmetric fission barrier and the elongation of the system at contact,[14] will require further experimental and theoretical studies. To describe theoretically the complex fusion dynamics after capture, multi-dimensional models[31,34,35] are being developed. Their future application to fusion reactions leading to new super-heavy elements promises insights into possible advantages of using short-lived neutron-rich nuclei, for which extensive experimental surveys will not be practicable.

5. Conclusions

A large static deformation of the heavy partner in a nuclear collision has been demonstrated to affect the probability of quasi-fission. Experimental data indicate that collisions at the lowest beam energies that result in contact between projectile and target favour quasi-fission, and thus must inhibit true fusion. This is related to the elongation of the combined system, and the low frequency of the collective rotational motion which is induced. In contrast, collisions involving heavy spherical nuclei show no evidence of enhancement of quasi-fission at low beam energies, which is argued to be due to the high frequencies of the collective vibrations excited during the collision.

The comprehensive data set obtained for three mass-asymmetric reactions leading to the compound nucleus ^{216}Ra indicates that the mass-asymmetry affects the probability of quasi-fission already for extremely asymmetric reactions (^{19}F + ^{197}Au), even at low angular momenta. These experimental results provide a quantitative test of the physics incorporated in theoretical models of ER formation, through focusing on the boundary between the simple fusion process envisaged by Bohr, and the complex and delicate dynamical process required to coax two heavy nuclei together.

Acknowledgement. M.D. acknowledges the support of an Australian Research Council QEII Fellowship.

References

(1) S. Hofmann and G. Münzenberg, Rev. Mod. Phys. **72**, 733 (2000), and references therein.
(2) Yu. Ts. Oganessian, A. V. Yeremin, A. G. Popeko, S. L. Bogomolov, G. V. Buklanov, M. L. Chelnokov, V. I. Chepigin, B. N. Gikal, V. A. Gorshkov, G. G. Gulbekian, M. G. Itkis, A. P. Kabachenko, A. Yu. Lavrentev, O. N. Malyshev, J. Rohac, R. N. Sagaidak, S. Hofmann, S. Saro, G. Giardina, and K. Morita, Nature **400**, 242 (1999).
(3) Yu. Ts. Oganessian, V. K. Utyonkov, Yu. V. Lobanov, F. Sh. Abdullin, A. N. Polyakov, I. V. Shirokovsky, Yu. S. Tsyganov, G. G. Gulbekian, S. L. Bogomolov, B. N. Gikal, A. N. Mezentsev, S. Iliev, V. G. Subbotin, A. M. Sukhov, O. V. Ivanov, G. V. Buklanov, K. Subotic, M. G. Itkis, K. J. Moody, J. F. Wild, N. J. Stoyer, M. A. Stoyer, R. W. Lougheed, C. A. Laue, Ye. A. Karelin, and A. N. Tatarinov, Phys. Rev. C **63**, 011301(R) (2001).
(4) C. H. Dasso, S. Landowne, and A. Winther, Nucl. Phys. A **405**, 381 (1982); **407**, 221 (1993).
(5) N. Rowley, G. R. Satchler, and P. H. Stelson, Phys. Lett. B **254**, 25 (1991).
(6) J. R. Leigh, M. Dasgupta, D. J. Hinde, J. C. Mein, C. R. Morton, R. C. Lemmon, J. P. Lestone, J. O. Newton, H. Timmers, and J. X. Wei, Phys. Rev. C **52**, 3151 (1995).
(7) A. M. Stefanini, D. Ackermann, L. Corradi, D. R. Napoli, C. Petrache, P. Spolaore, P. Bednarczyk, H. Q. Zhang, S. Beghini, G. Montagnoli, L. Mueller, F. Scarlassara, G. F. Segato, F. Soramel, and N. Rowley, Phys. Rev. Lett. **74**, 864 (1995).
(8) C. R. Morton, M. Dasgupta, D. J. Hinde, J. R. Leigh, R. C. Lemmon, J. P. Lestone, J. C. Mein, J. O. Newton, H. Timmers, N. Rowley, and A. T. Kruppa, Phys. Rev. Lett. **72**, 4074 (1994).
(9) M. Dasgupta, D. J. Hinde, N. Rowley, and A. M. Stefanini, Ann. Rev. Nucl. Part. Sci. **48**, 401 (1998).
(10) W. D. Myers and W. J. Swiatecki, Phys. Rev. C **62**, 044610 (2000).
(11) B. B. Back, R. R. Betts, J. E. Gindler, B. D. Wilkins, S. Saini, M. B. Tsang, C. K. Gelbke, W. G. Lynch, M. A. McMahan, and P. A. Baisden, Phys. Rev. C **32**, 195 (1985).
(12) W. Q. Shen, J. Albinski, A. Gobbi, S. Gralla, K. D. Hildenbrand, N. Herrmann, J. Kuzminski, W. F. J. Muller, H. Stelzer, J. Toke, B. B. Back, S. Bjornholm, and S. P. Sorensen, Phys. Rev. C **36**, 115 (1987).
(13) D. J. Hinde, M. Dasgupta, J. R. Leigh, J. C. Mein, C. R. Morton, J. O. Newton, and H. Timmers, Phys. Rev. Lett. **74**, 1295 (1995).
(14) D. J. Hinde, M. Dasgupta, J. R. Leigh, J. C. Mein, C. R. Morton, J. O. Newton, and H. Timmers, Phys. Rev. C **53**, 1290 (1996).
(15) J. P. Lestone, A. A. Sonzogni, M. P. Kelly, and R. Vandenbosch, Phys. Rev. C **56**, R2907 (1997).
(16) J. C. Mein, D. J. Hinde, M. Dasgupta, J. R. Leigh, J. O. Newton, and H. Timmers, Phys. Rev. C **55**, R995 (1997).

(17) S. Mitsuoka, H. Ikezoe, K. Nishio, and J. Lu, Phys. Rev. C **62**, 054603 (2000).
(18) K. Nishio, H. Ikezoe, S. Mitsuoka, and J. Lu, Phys. Rev. C **62**, 014602 (2000).
(19) C.-C. Sahm, H.-G. Clerc, K.-H. Schmidt, W. Reisdorf, P. Armbruster, F. P. Hessberger, J. G. Keller, G. Münzenberg, and D. Vermeulen, Nucl. Phys. A **441**, 316 (1985).
(20) R. L. Hahn, K. S. Toth, Y. LeBeyec, B. Lagarde, and M. W. Guidry, Phys. Rev. C **36**, 2132 (1987).
(21) A. C. Berriman, D. J. Hinde, M. Dasgupta, C. R. Morton, R. D. Butt, and J. O. Newton, Nature **413**, 144 (2001).
(22) C. R. Morton, D. J. Hinde, J. R. Leigh, J. P. Lestone, M. Dasgupta, J. C. Mein, J. O. Newton, and H. Timmers, Phys. Rev. C **52**, 243 (1995).
(23) N. Bohr, Nature **137**, 344 (1936).
(24) J. P. Lestone, J. R. Leigh, J. O. Newton, D. J. Hinde, J. X. Wei, J. X. Chen, S. Elfstrom, and M. Zielinska-Pfabe, Nucl. Phys. A **559**, 277 (1993).
(25) P. Vergani, E. Gadioli, E. Varciago, E. Fabrici, E. Gadioli Erba, M. Galmarini, G. Ciavola, and C. Marchetta, Phys. Rev. C **48**, 1815 (1993), and references therein.
(26) N. Rowley, J. R. Leigh, J. X. Wei, and R. Lindsay, Phys. Lett. B **314**, 179 (1993).
(27) A. B. Balantekin, A. J. DeWeerd, and S. Kuyucak, Phys. Rev. C **54**, 1853 (1996).
(28) J. Toke, R. Bock, G. X. Dai, A. Gobbi, S. Gralla, K. D. Hildenbrand, J. Kuzminski, W. J. F. Muller, A. Olmi, H. Stelzer, B. B. Back, and S. Bjornholm, Nucl. Phys. A **440**, 327 (1985).
(29) V. S. Ramamurthy, S. S. Kapoor, R. K. Choudhury, A. Saxena, D. M. Nadkarni, A. K. Mohanty, B. K. Nayak, S. V. Sastry, S. Kailas, A. Chatterjee, P. Singh, and A. Navin, Phys. Rev. Lett. **65**, 25 (1990).
(30) G. V. Ravi Prasad and V. S. Ramamurthy, Phys. Rev. C **54**, 815 (1996).
(31) G. G. Adamian, N. V. Antonenko, and W. Scheid, Nucl. Phys. A **678**, 24 (2000), and references therein.
(32) K. T. R. Davies and A. J. Sierk, Phys. Rev. C **31**, 915 (1985).
(33) P. Möller and J. R. Nix, Nucl. Phys. A **281**, 354 (1977).
(34) Y. Aritomo, T. Wada, M. Ohta, and Y. Abe, Phys. Rev. C **59**, 796 (1999).
(35) V. I. Zagrebaev, Phys. Rev. C **64**, 034606 (2001).